文章编号:1001-9014(2007)06-0401-04

ANALYSIS OF FILTER CHARACTERISTICS FOR A NEW DIELECTRIC GRATING WAVEGUIDE

PAN Yong-Mei, XU Shan-Jia

(Department of Electronics Engineering and Information Science,
University of Science & Technology of China, Hefei 230027, China)

Abstract: A new stopband filter consisted of dielectric grating waveguide was proposed and its filter characteristics were carefully examined by an approach of combining the multimode network theory with the rigorous mode-matching method. The Brillouin diagram for the dominant TM mode and the variations of the normalized center frequency and the band width as well as the maximum attenuation constant of the stopband with the geometry parameters were presented. By comparing with the traditional dielectric grating stopband filter, it has been found that the new filter structure not only has the advantage of lower conductor loss, but also is of larger stopband bandwidth and maximum attenuation in the band than those of the traditional ones. The numerical results presented here are of guiding significance for the design of new band-rejected filters.

Key words: periodically corrugated dielectric waveguide; mode-matching method; filter characteristics

CLC number: TN814 **Document**: A

一种新型介质栅波导滤波特性的研究

潘咏梅, 徐善驾

(中国科学技术大学 电子工程与信息科学系,安徽 合肥 230027)

摘要:提出了一种新型介质栅波导阻带滤波结构,并采用多模网络与严格模匹配相结合的方法对该阻带滤波特性进行了仔细分析,给出了主模TM模的Brillouin图及滤波结构的归一化中心频率、阻带的宽度和带内最大衰减等特性和结构参数的关系.与传统的介质栅滤波器相比,新滤波器结构不仅具有金属损耗小的优点,而且其阻带带宽和带内衰减都要比传统介质栅滤波器的大得多.文中所给出的计算结果对设计该新型带阻滤波结构有指导意义.

关 键 词:周期扰动介质波导;模匹配方法;滤波特性

Introduction

The dielectric periodic structure has shown substantial promise as a filter or leaky-wave antenna for millimeter-wave applications. This is because the structure is easy for fabrication; and can be conveniently connected with other components in the millimeter-wave integrated circuit so that the cost, size and weight of the system can be greatly reduced. Just for these reasons, strong interest in researching this kind of structure appears in the literature[1~9].

In this paper, a new grating filter configuration, presented in Fig. 1 (a), is investigated, which is of similar constituent structure to the traditional one as shown in Fig. 1 (b). The only difference between the two filters is the location of the planar layer and the grating layer to be exchanged from each other, namely, the whole part of the structure above the ground plane is inverted. Fig. 1 (c) shows the periodic corrugations for the new filter. Since the effective dielectric constant of the planar layer is grater than that of the grating layer, the fields decay exponentially in the grating layer with most of the energy confined to the planar layer. Consequently, compared with the traditional grating

Received date: 2007-03-22, **revised date**: 2007-08-15 **收稿日期**:2007-03-22, **修回日期**:2007-08-15

Foudantion item: Supported by National Natural Science Foundations of China(60471037,60531020)

Biography: PAN Yong-Mei (1982-), female, Hefei, China, Ph. D. candidate. Research field is restraint and utilization of leaky wave.

configuration, the new one has a virtue of lower conductor loss.

The coupling effect between n = 0 space harmonic of forward waves and n = −1 space harmonic of backward waves of the new periodically corrugated dielectric waveguide is carefully examined by an approach of combining the multimode network theory with the rigorous mode-matching method. Meanwhile, the Brillouin diagram for the fundamental TM mode is given with a comparison for the dispersion characteristics between the present and traditional filters. Also the normalized center frequency, the bandwidth and the maximum attenuation constant in the stopband are numerically presented as a function of the structure parameters.

1 Analyses

The schematics of the grating structures under consideration are shown in Fig. 1(a) and (b) respectively. The former is the proposed new filter structure, and the later is traditional one. Both structures consist of several parts, including feeder, taper, and the periodic corrugation. The taper is a corrugated transition section with the periodic layer thickness decreased (increased for the traditional one) gradually in order to reduce the input voltage standing-wave ratio (VSWR). The periodic corrugation, taking the present new filter as an example, is shown in Fig. 1 (c), which can be divided into three regions: region I, the outer free space; region II, the planar layer and region III, dielectric-air periodic layer. The periodic corrugation of the traditional filter is similar with the new one, therefore the detail description is omitted here for simplicity.

The dispersion characteristics or the Brillouin diagram of the dominant TM mode in the new and traditional periodic structures are investigated by combining the multimode network theory with the rigorous mode matching procedure. Due to the spatial periodicity of the grating layer in the x direction, all space harmonics are generally excited everywhere in the whole structure; the eigenfunctions in the air and planar layer regions should be represented by infinite number of transmission lines, each of which stands for one space harmonic. The whole filter structure can then be described

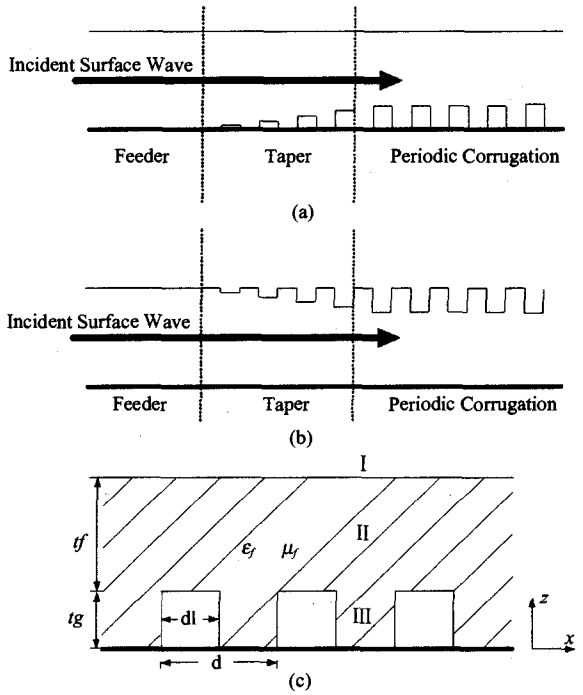

Fig. 1 (a) Configuration of new grating filter structure (b) configuration of traditional grating filter structure (c) periodic corrugations for new filter structure $\varepsilon_f = 2.1, \mu_f = 1$

图1 (a)新型介质栅滤波器结构(b)传统介质栅滤波器结构(c)新滤波器中的周期结构

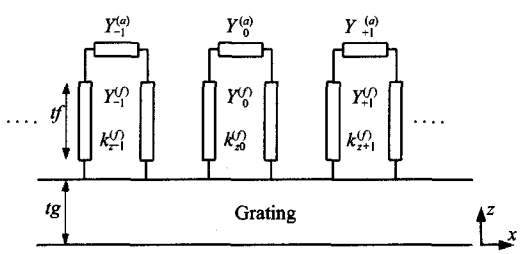

Fig. 2 Equivalent multimode network representation

图2 等效多模网络

by the multimode network as given in Fig. 2.

The admittance matrix $\mathbf{Y}_a$ looking into the air region, is a diagonal matrix

$$\mathbf{Y}_a = (\delta_{nl} Y_n^{(a)}) \quad , \tag{1}$$

where

$$Y_n^{(a)} = \begin{cases} k_{zn}^{(a)}/\omega\mu_0 & \text{for TE mode} \\ \omega\varepsilon_0/k_{zn}^{(a)} & \text{for TM mode} \end{cases} ,$$

$$k_{zn}^{(a)2} = k_0^2 - k_{xn}^2 \quad ,$$

$$k_{xn} = k_{x0} + 2n\pi/d \quad ,$$

Consequently, at the $z = tg$ interface, the admittance matrix $\mathbf{Y}_{up}$, looking up into the uniform planar region is given by the following transfer relationship:

$$\mathbf{Y}_{up} = \mathbf{Y}_f[\mathbf{1} - \mathbf{H}\Gamma_f\mathbf{H}][\mathbf{1} + \mathbf{H}\Gamma_f\mathbf{H}]^{-1} \quad , \quad (2)$$

where

$$\Gamma_f = [\mathbf{Y}_f + \mathbf{Y}_\alpha]^{-1} \cdot [\mathbf{Y}_f - \mathbf{Y}_\alpha]$$

$$(\mathbf{H})_{mn} = \delta_{mn}\exp(-jk_{zn}^{(f)}tf) \quad ,$$

The key step to the boundary value problem is the construction of a general solution for the periodic region, which has been well established in[10,11]. Thus, we can obtain the input admittance matrix $\mathbf{Y}_{dn}$, at z = tg interface, looking down into the grating region

$$\mathbf{Y}_{up} = \mathbf{I}[\mathbf{1} - e^{-jktg}\Gamma e^{-jktg}][\mathbf{1} + e^{-jktg}\Gamma e^{-jktg}]^{-1}(\mathbf{V})^{-1} \quad , \quad (3)$$

where $\Gamma = -\mathbf{1}$ is the reflection coefficient for the ground perfect conductor. Therefore, the complex eigenvalue of the boundary value problem can be finally solved by the generalized transverse resonance condition at z = tg interface,

$$\det[\mathbf{Y}_{up} + \mathbf{Y}_{dn}] = 0 \quad . \quad (4)$$

The determinant equation (4) defines the dispersion relation that is exact in principle. However it involves an infinite determinant; hence it has to be truncated for a numerical analysis. In the present calculations the truncation number of M = N = 8 is employed in the mode matching procedure, and the solution convergence is guaranteed by checking the numerical results carefully.

3 Numerical Results

Fig. 3 shows the typical Brilliouin diagrams of the periodic structure excited with TM fundamental mode, in which the enlarged dispersion curve at the vicinity of the stopband is also shown. In this figure the solid line stands for the numerical results for the present filter, while the dash line presents the data for the traditional one. As expected, the Bragg reflection occurs at βd = π, for $k_z = \beta - j\alpha$ is complex in the frequency region. This stopband characteristic results from the coupling between $n = 0$ forward space harmonic and $n = -1$ backward space harmonic waves. This property can be applied to make band-rejection filters. Seen from the figures, it is clear that the stopband bandwidth and maximum attenuation of the new periodic structure are much larger than those of the traditional one. The maximum attenuation is at least one order larger and stopband bandwidth about eight times wider. It is easy to

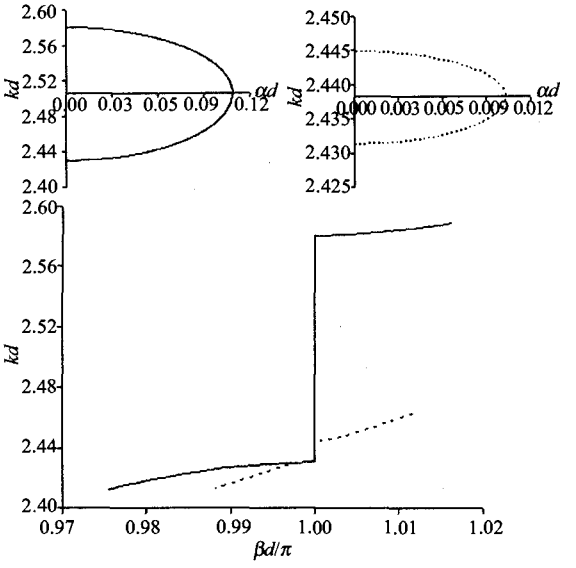

Fig. 3 Comparison of Brillouin diagram for the fundamental TM mode in the grating guide between the present and traditional filters (tf = 8e − 3; tg = 2e − 3; d = 12e − 3; $d1$ = 0.5d)
图 3　新的和传统的介质栅波导中主模 Brillouin 图的比较

be understood, since the fields in the grating layer are much stronger in the new structure. As a result, the coupling effect between the space harmonics is enhanced. It is noted that the abscissas of the attenuation curves are different for two filters.

The effect of grating thickness tg on the normalized center frequency $(kd)_c$, band-width $(\Delta kd)/(kd)_c$ and the maximum attenuation constant $(\alpha d)_c$ in the stopband is presented in Fig. 4. It is found that with the increment of tg, the band-width $(\Delta kd)/(kd)_c$ and the maximum attenuation constant $(\alpha d)_c$ in-

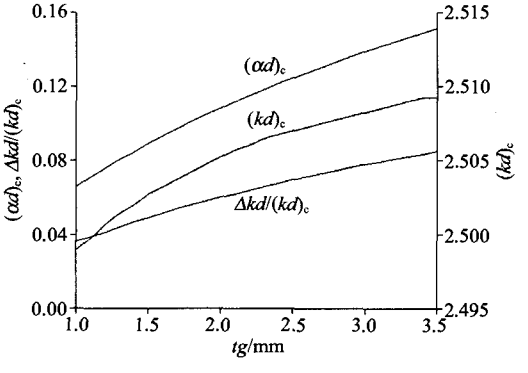

Fig. 4 Effect of grating thickness on the normalized center frequency, band-width and the maximum attenuation constant of the stopband. (tf = 8e − 3; d = 12e − 3; $d1$ = 0.5d)
图 4　栅高对介质栅波导主模阻带归一化中心频率、带宽和最大衰减常数的影响

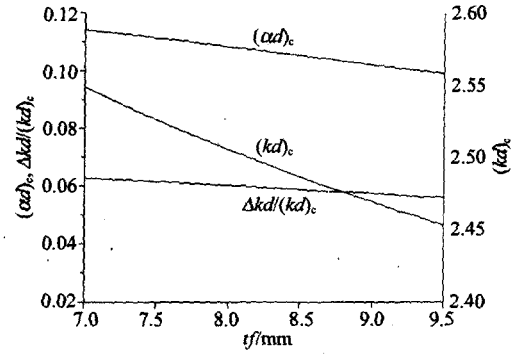

Fig. 5 Effect of planar layer thickness on the normalized center frequency, band-width and the maximum attenuation constant of the stopband($tg=2e-3$; $d=12e-3$; $d1=0.5d$)

图5 平板厚度对介质栅波导主模阻带归一化中心频率、带宽和最大衰减常数的影响

crease rapidly, so does the normalized center frequency $(kd)_c$. This is because the lager the tg, the fields are more distributed in the grating layer, which results in smaller effective dielectric constant and leads to the ascending of the normalized center frequency $(kd)_c$. For the same reason, the coupling between space harmonics becomes stronger.

Fig. 5 shows the effect of planar layer thickness *tf* on the normalized center frequency $(kd)_c$, the normalized maximum attenuation $(\alpha d)_c$ and the normalized band-width $(\Delta kd)/(kd)_c$ of the stopband. It is found that with the increment of the thickness *tf*, the normalized center frequency $(kd)_c$ descends rapidly, this is because with the increment of the thickness *tf*, the fields are more concentrated in the plane layer and the effective dielectric constant becomes larger; at the same time, as the increasing of *tf*, the normalized maximum attenuation $(\alpha d)_c$ of the stopband also descending rapidly, but the descending of $(\Delta kd)/(kd)_c$ is not so sensitive as $(kd)_c$ and $(\Delta kd)/(kd)_c$ are. It is believed that these curves provide useful guidelines for the design of the present band-rejection filter.

3 Conclusion

In this paper, the filter properties of a new periodic corrugation are analyzed with the rigorous mode matching method . The variations of the normalized center frequency; bandwidth and maximum attenuation constant of the stopband with geometry parameters are carefully investigated. It has been found that the new filter not only has the advantage of lower conductor loss, but also is of much larger stopband bandwidth and maximum attenuation than those of the traditional ones. Based on the analysis, some useful guidelines for the filter design are thereby suggested.

REFERENCES

[1] Schwering P K, Peng S T. Design of Dielectric grating antennas for millimeter wave applications[J]. *IEEE Trans. on MTT.*, 1993, **31**: 199—209.

[2] Itoh T. Applications of grating in a dielectric waveguide for leaky-wave antennas and band-reject filters [J]. *IEEE Trans. on MTT.*, 1977, **25**: 1134—1138.

[3] Jing Hengzhen, Xu Shanjia, Wu Xianliang. Analysis of filter characteristics for a circular periodically corrugated dielectric rod waveguide with mode matching method[J]. *Chinese Journal of Electronics*, 2003, **12**(2): 302—304.

[4] Goussetis G, Feresidis A P. Kosmas P. Efficient analysis, design, and filter applications of EBG waveguide with periodic resonant loads [J]. *IEEE Trans. on MTT.*, 2006, **54**(11): 3885 3892.

[5] Cameron R J, Ming Yu, Ying Wang. Direct-coupled microwave filters with single and dual stopbands [J]. *IEEE Trans. on MTT.*, 2005, **53**(11): 3288— 3297.

[6] Catina V, Arndt F, Brandt J. Hybrid surface integral-equation/mode-matching method for the analysis of dielectric loaded waveguide filters of arbitrary shape [J]. *IEEE Trans. on MTT.*, 2006, **12**: 3562—3567.

[7] Chih-Ming Tsai, Hong-Ming Lee, Chin-Chuan Tsai. Planar filter design with fully controllable second passband [J]. *IEEE Trans. on MTT.*, 2006, **54**(12): 3429—3439.

[8] TIAN Jia-Sheng, LI Xin, SHI Jian, *et al.* Analysis of Characteristics of wave Propogation in dielectric waveguide array [J]. *J. Infrared Millim. Waves*(田加胜,李昕,石坚,等. 介质波导电磁特性分析. **红外与毫米波学报**), 2005, **24**(2): 156—160.

[9] CHENG Jian, XU Shan-Jia, WU Ke. Theoretical analysis of a new grating leaky wave antenna based on left-handed materials[J]. *J. Infrared Millim. Waves*(程健,徐善驾,吴柯. 一种基于左手介质的新型介质栅漏波天线的理论分析. **红外与毫米波学报**), 2007, **26**(5): 321—325.

[10] Xu Shanjia, Zheng Fenghua. Multimode network analysis for dielectric leaky-wave antennas consisting of multilayer periodic structure with arbitrary dielectric distributions[J]. *Int. J. Infrared Millim. Waves*, 1997, **18**(6): 1223—1240.

[11] WU Zhan-Zhan, XU Shan-Jia. Rigorous mode matching analysis of transmission characteristics for periodic dielectric structures[J]. *J. Infrared Millim. Waves*(伍瞻瞻,徐善驾. 周期介质结构传输特性的严格模匹配分析. **红外与毫米波学报**), 2004, **23**(1): 21—26.